Proc. Natl. Acad. Sci. USA
Vol. 92, pp. 10914–10918, November 1995
Biochemistry

Multiple calcium channel transcripts in rat osteosarcoma cells: Selective activation of α_{1D} isoform by parathyroid hormone

ELIZABETH L. R. BARRY*†, FRANK A. GESEK*, STANLEY C. FROEHNER‡, AND PETER A. FRIEDMAN*

*Department of Pharmacology and Toxicology, Dartmouth Medical School, Hanover, NH 03755-3835; and ‡Department of Physiology, University of North Carolina, Chapel Hill, NC 27599-7545

Communicated by Philip Needleman, Monsanto Company, St. Louis, MO, July 17, 1995 (received for review January 18, 1995)

ABSTRACT **Osteoblasts express calcium channels that are thought to be involved in the transduction of extracellular signals regulating bone metabolism. The molecular identity of the pore-forming subunit (α_1) of L-type calcium channel(s) was determined in rat osteosarcoma UMR-106 cells, which express an osteoblast phenotype. A homology-based reverse transcriptase–polymerase chain reaction cloning strategy was employed that used primers spanning the fourth domain. Three types of cDNAs were isolated, corresponding to the α_{1S} (skeletal), α_{1C} (cardiac), and α_{1D} (neuroendocrine) isoforms. In the transmembrane segment IVS3 and the extracellular loop formed by the IVS3–S4 linker, a single pattern of mRNA splicing was found that occurs in all three types of calcium channel transcripts. Northern blot analysis revealed an 8.6-kb mRNA that hybridized to the α_{1C} probe and 4.8- and 11.7-kb mRNAs that hybridized to the α_{1S} and α_{1D} probes. Antisense oligonucleotides directed to the calcium channel α_{1D} transcript, but not those directed to α_{1S} or α_{1C} transcripts, inhibited the rise of intracellular calcium induced by parathyroid hormone. However, α_{1D} antisense oligonucleotides had no effect on the accumulation of cAMP induced by parathyroid hormone. When L-type calcium channels were activated with Bay K 8644, antisense oligonucleotides to each of the three isoforms partially inhibited the rise of intracellular calcium. The present results provide evidence for the expression of three distinct calcium channel α_1-subunit isoforms in an osteoblast-like cell line. We conclude that the α_{1D} isoform is selectively activated by parathyroid hormone.**

Voltage-gated calcium (Ca^{2+}) channels were first described in excitable cells and are generally classified as L, N, P, and T type (1). L-type Ca^{2+} channels are defined by their high-voltage-dependent activation and by their sensitivity to organic Ca^{2+} channel blockers, including dihydropyridines (2). Ca^{2+} channels are multimeric complexes whose properties are largely conferred by the pore-forming α_1 subunit, which contains four homologous domains, each with six putative transmembrane regions (S1–S6). At least six Ca^{2+} channel α_1 subunit genes have been identified including three L-type isoforms (3). Additional diversity of Ca^{2+} channel structure is generated by alternative splicing, which gives rise to multiple transcripts from each gene.

Osteoblasts play a central role in the regulation of bone metabolism because they are responsible for bone formation and modulate bone resorption by osteoclasts. Parathyroid hormone (PTH), the principal hormone regulating serum Ca^{2+}, causes a rapid Ca^{2+} influx into osteoblasts through plasma membrane Ca^{2+} channels (4, 5). The Ca^{2+} signals generated are likely to be involved in the induction of intracellular responses that regulate bone turnover (6). The pharmacological and kinetic characteristics of osteoblast Ca^{2+} channels resemble those of L-type voltage-gated Ca^{2+} channels expressed in excitable cells (7–12).

The purpose of the present study was to determine the molecular identity of L-type Ca^{2+} channels expressed in UMR-106 osteoblast-like cells and to examine their regulation by PTH. Three types of cDNA clones were isolated corresponding to all three isoforms of L-type voltage-gated Ca^{2+} channels that have been described in excitable cells.§ A rare pattern of alternative splicing was found to occur in all three types of transcripts. Antisense oligonucleotides (ODNs) were used to demonstrate that PTH selectively activates the α_{1D} isoform. Some of these results have been presented (13).

EXPERIMENTAL PROCEDURES

cDNA Synthesis and PCR. UMR-106 cells (14) were obtained from American Type Culture Collection and were cultured in Dulbecco's modified Eagle's medium/Ham's F-12 medium (Sigma) containing 10% (vol/vol) fetal bovine serum (Sigma). Poly(A)$^+$ RNA was isolated from cultured cells by using the FastTrack mRNA isolation kit (Invitrogen). Reverse transcription and cDNA amplification were carried out with the GeneAmp RNA PCR kit (Perkin–Elmer/Cetus) on 250 ng of poly(A)$^+$ RNA. Thirty cycles of PCR were performed: 60 s at 94°C, 60 s at 60°C, and then 120 s plus 2 s per cycle at 72°C. PCR primer ODNs (Macromolecular Resources, Fort Collins, CO) were designed to amplify essentially the entire fourth domain by using regions that are highly conserved between the α_1 subunit of L-type Ca^{2+} channels in published sequences: α_{1S} (rabbit skeletal muscle isoform) (15), α_{1C} (rat cardiac muscle isoform) (16), and α_{1D} (rat neuroendocrine isoform) (17). The upstream primer was 5′-GCCGGATCCATCGTCACCTTC-CAGGAGCA-3′, and the downstream primer was 5′-ATG-GAATTCGCCACRAAGAGGTTGATGAT-3′ (R = A or G). An additional downstream primer, 5′-CCCGAATTCAK-MGTGTTGAGCATGATGAG-3′ (K = T or G; M = A or C), was designed from sequence in the IVS1 segment (residues 167–195) of the UMR-106 ROB1 and ROB3 rat osteoblast clones to be used with the upstream primer to amplify only the 5′ end of those clones. *Bam*HI or *Eco*RI restriction sites (underlined) were included near the 5′ ends of the primers to facilitate directional subcloning.

Cloning and Sequencing PCR Products. The PCR products were directionally cloned into the pBluescript KS− vector (Stratagene). For sequencing, 5 μg of plasmid DNA was denatured in 200 mM NaOH/0.2 mM EDTA for 30 min at 37°C, neutralized, and precipitated in ethanol. Sequencing was performed by the dideoxynucleotide chain-termination method with the Sequenase II kit (United States Biochemical). The products were separated by electrophoresis on 8.0% polyacrylamide gels (Gel-Mix 8, GIBCO/BRL). The final

The publication costs of this article were defrayed in part by page charge payment. This article must therefore be hereby marked "*advertisement*" in accordance with 18 U.S.C. §1734 solely to indicate this fact.

Abbreviations: $[Ca^{2+}]_i$, intracellular calcium activity; ODNs, oligodeoxynucleotides; PTH, parathyroid hormone.

†To whom reprint requests should be addressed.

§The sequences reported in this paper have been deposited in the GenBank data base (accession nos. U31772, U31815, and U31816).

sequences were determined from both strands of the cDNA. Sequence analysis was performed with on-line software from the Genetics Computer Group (Madison, WI).

Northern Blot Analysis. Poly(A)$^+$ RNA was electrophoresed on a 0.75% agarose/formaldehyde denaturing gel and electrophoretically transferred to GeneScreen*Plus* nylon membrane (DuPont/NEN). The membranes were UV-crosslinked and baked for 2 h at 80°C under vacuum. Prehybridization was carried out in 0.25 M sodium phosphate/pH 7.2/0.25 M NaCl/1 mM EDTA/50% (vol/vol) formamide/6% (wt/vol) SDS at 55°C for 1 h. ^{32}P-labeled RNA probes were synthesized by using [α-^{32}P]UTP (Amersham), linearized cDNA templates and the Riboprobe Gemini System (Promega). After hybridization with RNA probes, 2×10^6 cpm/ml, the membranes were washed and incubated with RNase A (1 μg/ml) for 15 min at room temperature. Final high-stringency washes were in 0.04 M sodium phosphate, pH 7.2/1% SDS/1 mM EDTA at 65°C.

Antisense Analysis. ODNs were introduced into UMR-106 cells during permeabilization with streptolysin O (GIBCO/BRL) as described (18), with the following modifications. Cells in suspension were incubated with streptolysin O (20 units/ml) for 10 min at 37°C in the presence of 100 μM ODNs (sense or antisense). Control cells were permeabilized in the absence of ODNs. Cells were then washed and plated onto glass coverslips. After 18–24 h, intracellular calcium activity ($[Ca^{2+}]_i$) was measured in single cells loaded with fura-2 (Molecular Probes) as described (19). Antisense ODNs were designed from regions of sequences that are divergent between the three Ca^{2+} channel isoforms to be highly specific: α_{1S}, 5′-TTCCCG-TAGCTGCAGGCCAG-3′; α_{1C}, 5′-CCTTCCGTGCTGTT-GCTGGGCTCA-3′; α_{1D}, 5′-ATCTGGTTGTTATCTCT-CAT-3′. The dose of ODNs used (100 μM) and amount of time after ODN treatment (18–24 h) before assaying for functional inhibition of Ca^{2+} channel activity have been found to be maximally inhibitory for the α_{1C} Ca^{2+} channel protein (18).

Measurement of cAMP. UMR-106 cells in suspension were incubated for 15 min at 37°C in the presence or absence of 1×10^{-8} M bovine PTH-(1–84) prior to the addition of ice-cold 0.132 M trichloroacetic acid. The supernatant was extracted with ether, dried, and used for the measurement of cAMP with a kit from Diagnostic Products (Los Angeles).

Statistical Analysis. Comparisons between control and experimental treatment groups were evaluated by analysis of variance (ANOVA) and post hoc analysis of multiple comparisons using the Bonferroni method (INSTAT; Graph-Pad Software, San Diego). Values are the mean ± SEM; *n*, number of experiments. $P \leq 0.05$ was assumed to be significant.

RESULTS

Homology-based reverse transcriptase–PCR was used to identify transcripts for L-type Ca^{2+} channels in UMR-106 cells. Three types of cDNA clones were isolated, corresponding to all three of the known L-type Ca^{2+} channel genes. The α_{1S} isoform (ROB1), 844 bp, is 91% identical at the nucleotide level and 97% identical at the amino acid level to the rabbit skeletal muscle α_{1S} gene (15). In addition, there is a 57-bp deletion (19 amino acids) in the S3–S4 linker region (Fig. 1). The α_{1C} isoform (ROB2), 850 bp, is identical to the rat brain rbC-I transcript (16), except for a 33-bp (11 amino acids) deletion (Fig. 1) in the S3–S4 linker. Finally, the α_{1D} isoform (ROB3), 844 bp, is identical to the corresponding rat brain transcript (17) except for two 1-bp changes, one of which results in a conservative amino acid change, and a 45-bp (15 amino acid) deletion in the S3–S4 linker (Fig. 1). Partial sequencing of four additional α_{1S} clones and five α_{1D} clones indicated that they all had the same pattern of alternative splicing.

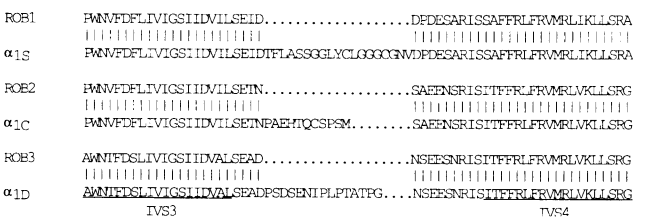

FIG. 1. Comparison of the deduced amino acid sequences of the UMR-106 clones with their corresponding calcium channel α_1 subunit isoforms in the region where alternative splicing generates a deletion. Comparisons: ROB1 to the rabbit skeletal muscle α_{1S} transcript (15); ROB2 to the rat brain α_{1C} transcript (16); ROB3 to the rat brain α_{1D} transcript (17).

Northern blot analysis was used to detect expression of mRNA transcripts corresponding to the UMR-106 Ca^{2+} channel clones (Fig. 2). Three sizes of mRNAs of approximately 11.7, 8.6, and 4.8 kb were detected. The ROB2 clone hybridized predominantly to the 8.6-kb mRNA, which is the expected size for an α_{1C} isoform transcript (16, 20, 21). However, a larger 12- to 15-kb transcript detected in other tissues (16, 20, 21), including cardiac muscle, aorta, and brain, was not seen. The ROB1 and the ROB3 clones hybridized to both the 4.8-kb (major) and 11.7-kb (minor) mRNAs. The size of the 11.7-kb transcript is similar to that reported (11.0 kb) for a human α_{1D} isoform isolated from pancreatic β cells (22). Interestingly, hybridization of the ROB1 clone to a 6.5-kb band, such as that seen in adult skeletal muscle (23), was not detected. However, the shorter transcript (4.8 kb) is similar in size to the predominant transcript reported in newborn skeletal muscle (24) and in kidney (25). Very high-stringency washing was used during Northern blot analysis to maximize the specificity of hybridization. Nevertheless, it is possible that the high degree of sequence identity (≈76%) of the three Ca^{2+} channel isoforms in the region cloned may be responsible for some cross-hybridization. In particular, the faint band at 4.8 kb detected by the ROB2 clone may be due to cross-hybridization by virtue of the relatively high abundance of those transcripts. In addition, the 8.6-kb band detected by ROB3 is likely to represent cross-hybridization since it was not labeled when a shorter ROB3 probe was used (data not shown).

The truncated (4.5 kb) transcript described in newborn muscle is generated by an internal deletion between IIS2 and IVS2 giving rise to an isoform with only two homologous domains (24). Northern blot analysis was used to examine whether a similar deletion is responsible for the shorter

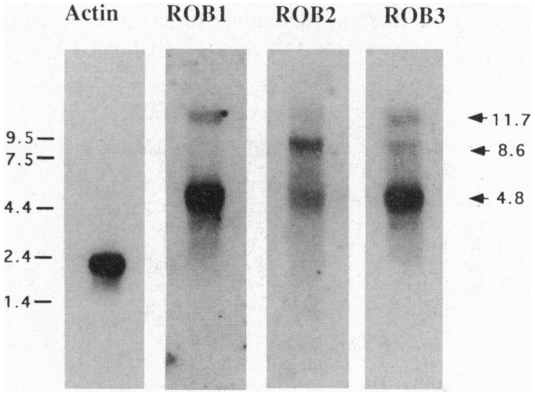

FIG. 2. Autoradiogram of a Northern blot of RNA hybridized to UMR-106 calcium channel α_1-subunit RNA probes. RNA probes were hybridized to UMR-106 poly(A)$^+$ RNA at 10 μg per lane for ROB1–ROB3 probes or at 1 μg per lane for the actin probe. Autoradiography was for 67 h (ROBs) or 6 h (actin). An RNA ladder (GIBCO/BRL) was used for size markers (in kilobases).

transcripts (4.8 kb) detected in UMR-106 cells with ROB1 and ROB3 probes. A downstream primer (DP-3) was designed from sequence in the IVS1 domain of the ROB1 and ROB3 cDNAs (corresponding to residues 167–195). This primer was used along with the upstream primer from IIIS6 to generate truncated cDNAs (225 bp) from ROB1 and ROB3, which contain only the IIIS6–IVS1 linker and a portion of IVS1. These cDNAs should not hybridize to the 4.8-kb mRNA from UMR-106 cells if it is formed by an internal deletion between IIS2 and IVS2. However, Northern blot analyses with either of the ROB1 or ROB3 truncated cDNAs as probes and with the full-length probes gave identical hybridization patterns (data not shown). These results indicate that the 4.8-kb mRNAs from UMR-106 cells are not formed by the same type of internal deletion reported for the 4.5-kb mRNA from newborn muscle.

Antisense analysis was used to examine which of the three L-type Ca^{2+} channel α_1 subunit isoforms is activated by PTH in UMR-106 cells. In control cells that were not treated with ODNs, PTH treatment caused $[Ca^{2+}]_i$ to rise rapidly to a new plateau (Fig. 3 and Table 1). However, in cells that had been treated with antisense ODNs to the Ca^{2+} channel α_{1D} isoform, the PTH-induced rise of $[Ca^{2+}]_i$ was significantly reduced to 36 ± 4% of the increase seen in control cells. Treatment of cells with α_{1D} sense ODNs or with sense or antisense ODNs to the α_{1S} or α_{1C} isoforms did not alter the magnitude of the PTH-induced rise of $[Ca^{2+}]_i$ relative to control cells (Table 1). Notably, basal $[Ca^{2+}]_i$ was not significantly changed by treatment of cells with any of the ODNs (data not shown). These results indicate that treatment of UMR-106 cells with PTH causes Ca^{2+} uptake through the selective activation of the Ca^{2+} channel α_{1D} isoform.

Antisense ODNs directed to the α_{1D} Ca^{2+} channel mRNA transcript are thought to reduce PTH-induced Ca^{2+} uptake by specifically inhibiting the expression of the α_{1D} Ca^{2+} channel protein. To rule out a nonspecific effect of α_{1D} antisense ODNs on the ability of UMR-106 cells to respond to PTH, increases of cAMP stimulated by PTH were measured ($n = 3$). In control cells, cAMP production increased 35-fold from a basal level of 10.7 ± 1.1 pmol/mg of protein in the absence of PTH to 375 ± 77 pmol/mg of protein in the presence of PTH. Neither basal nor PTH-stimulated cAMP formation was altered by treatment of the cells with α_{1D} sense (basal, 10.9 ± 1.0; +PTH, 356 ± 70 pmol/mg of protein) or antisense ODNs (basal, 10.8 ± 0.7; +PTH, 383 ± 33 pmol/mg of protein). Thus, α_{1D} antisense ODNs specifically inhibit Ca^{2+} uptake, but not the formation of cAMP, induced by PTH.

Treatment with antisense ODNs to the α_{1D} isoform only partially inhibited the PTH-induced rise of $[Ca^{2+}]_i$, suggesting that Ca^{2+} release from intracellular stores contributed to the rise of $[Ca^{2+}]_i$. To examine this possibility, the PTH-induced rise $[Ca^{2+}]_i$ was measured in the absence of extracellular Ca^{2+} or the presence of nifedipine, an L-type Ca^{2+} channel antagonist. In the absence of extracellular Ca^{2+}, the PTH-induced rise $[Ca^{2+}]_i$ was 57 ± 4% ($n = 4$) of the control value obtained in the presence of extracellular Ca^{2+}. Thus, a portion of the PTH-induced rise of $[Ca^{2+}]_i$ is due to release from intracellular stores. The effect of nifedipine on the PTH-induced rise of $[Ca^{2+}]_i$ was assessed in control cells and cells treated with α_{1D} ODNs (Fig. 4). Nifedipine significantly reduced the magnitude of the PTH-induced rise of $[Ca^{2+}]_i$ in control and sense-treated cells by ≈40%. However, nifedipine had no effect in cells treated with α_{1D} antisense ODNs. Notably, the PTH-induced rise of $[Ca^{2+}]_i$ in control and sense ODN-treated cells in the presence of nifedipine was similar in magnitude to that in α_{1D} antisense ODN-treated cells in the presence or absence of nifedipine. Thus, the inhibitory effects of nifedipine and α_{1D} antisense ODNs were similar in magnitude and not additive. These results demonstrate that the antisense ODNs and nifedipine inhibit the same component of the PTH-induced rise of $[Ca^{2+}]_i$, that attributable to the Ca^{2+} channel α_{1D} isoform.

The failure of the antisense ODNs to the α_{1S} or α_{1C} Ca^{2+} channel isoforms to inhibit the PTH-induced rise of $[Ca^{2+}]_i$ could potentially result from their failure to block the expression of their respective channel proteins. To rule out this possibility Bay K 8644, an L-type Ca^{2+} channel agonist, was used to stimulate channel activity directly. The rise of $[Ca^{2+}]_i$ induced by Bay K 8644 was compared in control cells and cells treated with antisense and sense ODNs to each of the three different Ca^{2+} channel isoforms (Fig. 5). Each of the antisense

Table 1. Summary of the effect of calcium channel ODNs on the PTH-induced rise of $[Ca^{2+}]_i$

Treatment	$\Delta[Ca^{2+}]_i$, % control	n
Control	100 ± 6	9
α_{1S} antisense	103 ± 9	6
α_{1S} sense	99 ± 18	3
α_{1C} antisense	102 ± 11	4
α_{1C} sense	82 ± 8	3
α_{1D} antisense	36 ± 4*†	9
α_{1D} sense	118 ± 16	6

$\Delta[Ca^{2+}]_i$, the difference between resting and stimulated level of $[Ca^{2+}]_i$ after 10^{-8} M PTH treatment. In control cells, the basal level of $[Ca^{2+}]_i$ was 119 ± 4 nM and the PTH-stimulated level was 243 ± 21 nM. The results are presented as the percent of the $\Delta[Ca^{2+}]_i$ obtained with control cells in the same set of experiments. *, $P < 0.01$, α_{1D} antisense vs. control; †, $P < 0.001$, α_{1D} antisense vs. α_{1D} sense.

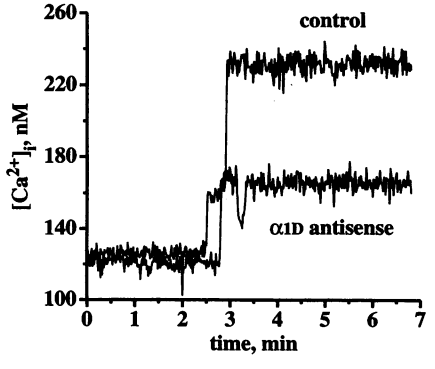

FIG. 3. Effect of α_{1D} (ROB3) antisense ODNs on the PTH-induced rise of intracellular calcium. Representative traces of $[Ca^{2+}]_i$ are shown for single cells in which basal $[Ca^{2+}]_i$ was measured for 2 min followed by exposure to 10^{-8} M PTH for 5 min.

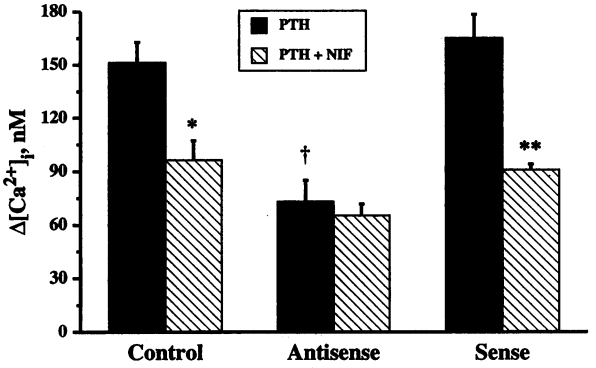

FIG. 4. Effect of nifedipine on the PTH-induced rise of intracellular calcium. $\Delta[Ca^{2+}]_i$, the difference between resting and stimulated levels of $[Ca^{2+}]_i$ after treatment with 10^{-8} M PTH. In some experiments, nifedipine (NIF, 10 μM) was present. In control cells, the basal level of $[Ca^{2+}]_i$ was 124 ± 2 nM and the PTH-stimulated level was 280 ± 12 nM ($n = 6$). *, $P < 0.05$, control PTH + NIF vs. control PTH; †, $P < 0.05$, antisense PTH vs. control PTH; **, $P < 0.01$, sense PTH + NIF vs. sense PTH.

ODNs significantly reduced the magnitude of the Bay K 8644-induced rise of $[Ca^{2+}]_i$, whereas the corresponding sense ODNs had no effect. These results provide functional evidence that the α_{1S}, α_{1C}, and α_{1D} antisense ODNs are effective inhibitors of Ca^{2+} channel gene expression.

DISCUSSION

Previous studies of Ca^{2+} channels in osteoblast-like cells (6, 7, 9, 11, 26) and normal rat osteoblasts (9, 12, 27) utilized electrophysiological techniques to provide evidence for the presence of L-type channels. However, it has not been clear whether more than one type of channel was present or what its relationship was to the Ca^{2+} channels described in excitable cells. In the present study, three α_1 subunit isoforms of L-type voltage-gated Ca^{2+} channels were found in UMR-106 osteoblast-like osteosarcoma cells. Each of these α_1 subunit transcripts (α_{1S}, α_{1C}, and α_{1D}) exhibits a specific pattern of alternative splicing in the fourth domain involving two adjacent regions. The first region is the IVS3 transmembrane domain in which mutually exclusive alternate exons can be used, as has been described in several different tissues including brain, heart, and aorta (for α_{1C}) and in brain (for α_{1D}) (17, 21, 28, 29). In each of these tissues both types of exons are expressed. However, in UMR-106 cells only one of the two types of exons was found, and it is the same type in each of the three Ca^{2+} channel transcripts.

The second region of alternative splicing is in the IVS3–S4 extracellular linker, wherein a deletion may result from exon skipping or the use of alternate splice acceptor sites. The presence of a deletion in this region has been found only rarely (25, 30, 31). This deletion was found to occur in the α_{1C} isoform at a low frequency (<12%) in many tissues (32). However, all of the Ca^{2+} channel α_1 subunit clones isolated from UMR-106 cells contained a deletion in this region. The combination of the specific IVS3 type found in UMR-106 cells and the deletion in the S3–S4 linker has been designated variant type b by Perez-Reyes *et al.* (30). Our results suggest that UMR-106 osteosarcoma cells express predominantly or exclusively the b variants of the α_{1S}, α_{1C}, and α_{1D} transcripts.

The functional effects and physiological roles for the two alternative splicing events that occur in the fourth domain are not known. The conservation of the splicing pattern between the three different Ca^{2+} channel α_1 subunit genes suggests the involvement of common cis- and/or transacting factors that regulate the mechanism of splicing. Splicing in this region may be responsible for similar functional effects in each of the Ca^{2+} channel proteins. Additional tissue-specific processing of the UMR-106 α_{1S} and α_{1D} transcripts is likely to occur since the size of the major transcript (4.8 kb) is significantly smaller than that reported from other sources (17, 22, 23). The nature of this difference is presently unknown. For the α_{1S} isoform, the existence of variants that have an internal deletion has been reported (24, 33). The present results, however, indicate that the osteosarcoma transcripts are not formed in a manner analogous to that described by Malouf *et al.* (24).

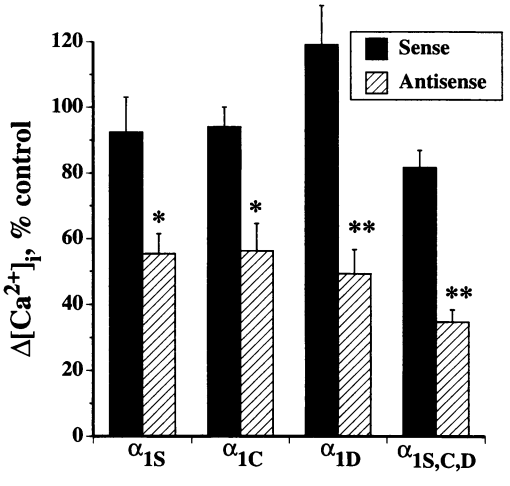

FIG. 5. Effect of calcium channel ODNs on the Bay K 8644-induced rise of intracellular calcium. $\Delta[Ca^{2+}]_i$, the difference between resting and stimulated levels of $[Ca^{2+}]_i$ after treatment with (*S*)-(−)-Bay K 8644 (10 μM). In control cells, the basal level of $[Ca^{2+}]_i$ was 122 ± 2 nM and the Bay K 8644-stimulated level was 232 ± 12 nM. The results are presented as the percent of the $\Delta[Ca^{2+}]_i$ obtained with control cells in the same set of experiments (n = 7). *, $P < 0.05$ antisense vs. sense; **, $P < 0.01$ antisense vs. sense.

Treatment of osteoblasts with PTH causes a rise of $[Ca^{2+}]_i$ that involves both Ca^{2+} release from intracellular stores and Ca^{2+} influx through L-type Ca^{2+} channels (4–6). In the present study, inhibition of specific Ca^{2+} channel isoforms with antisense ODNs was used to demonstrate that PTH selectively activates the α_{1D} isoform to cause Ca^{2+} uptake into UMR-106 cells. After exposure of cells to α_{1D} antisense ODNs, the PTH-induced rise of $[Ca^{2+}]_i$ was inhibited by 64% (Table 1). A similar reduction in the PTH-induced rise of $[Ca^{2+}]_i$ was obtained with nifedipine (Fig. 4) or upon removal of extracellular Ca^{2+}. Thus, the residual rise of $[Ca^{2+}]_i$ in cells treated with α_{1D} antisense ODNs is likely to be due to the mobilization of Ca^{2+} from intracellular stores. Antisense ODNs to the α_{1S} and α_{1C} isoforms had no effect on the PTH-induced rise of $[Ca^{2+}]_i$ (Table 1). In addition, the observation that nifedipine caused no further reduction in the PTH-induced rise of $[Ca^{2+}]_i$ in α_{1D} antisense-treated cells (Fig. 4) supports the conclusion that the α_{1D} isoform is the only L-type Ca^{2+} channel activated by PTH. However, Yamaguchi and coworkers (4, 34, 35) suggested that PTH sequentially activates two distinct Ca^{2+} channels in UMR-106 cells that appear to be regulated separately by second messenger systems involving either cAMP or protein kinase C. Although the present study provides evidence for activation of only one type of Ca^{2+} channel α_1 subunit (α_{1D}) by PTH, it is possible that functional differences may arise from alternatively spliced isoforms of α_{1D} or from the association of α_{1D} with multiple isoforms of accessory subunits (β). Finally, the α_{1D} antisense ODNs had no effect on PTH-induced synthesis of cAMP. These results emphasize the specificity of the inhibitory effect of the antisense ODNs and show that other PTH actions are not impaired.

Antisense ODNs directed to each of the three α_1-subunit isoforms inhibited the rise of $[Ca^{2+}]_i$ induced by Bay K 8644 (Fig. 5). These results provide independent confirmation of the inhibitory effect of the α_{1D} antisense ODNs on Ca^{2+} channel activity. In addition, they demonstrate that the antisense ODNs to the α_{1S} and α_{1C} isoforms effectively inhibit Ca^{2+} channel activity. Thus, the lack of an effect of the α_{1S} and α_{1C} antisense ODNs on PTH-induced Ca^{2+} uptake does not result from their failure to block expression of the channel proteins. It might be expected that the inhibitory effects of the three different antisense ODNs on the Bay K 8644-induced rise of $[Ca^{2+}]_i$ would be additive. However, each of antisense ODNs inhibited ≈45% of the rise of $[Ca^{2+}]_i$, and the inhibition was not significantly increased by the combination of all three ODNs (Fig. 5). These results suggest that cooperative interactions may occur between the different Ca^{2+} channel isoforms during activation by Bay K 8644, possibly involving protein–protein interactions or modulation by $[Ca^{2+}]_i$.

PTH acts on bone cells in a complex and as yet poorly understood manner that may cause anabolic or catabolic effects (36). The cellular response to PTH is likely to involve the interplay between Ca^{2+} and cAMP second messenger systems and the precise roles of these two systems remain to be dissected. Modifications of $[Ca^{2+}]_i$ may regulate gene transcription from specific promoters that contain Ca^{2+}-responsive elements. Recent studies demonstrate that in-

creases of $[Ca^{2+}]_i$ after activation of L-type Ca^{2+} channels regulate c-*fos* gene transcription in neuronal cells (37, 38) and that c-fos is an important modulator of osteoblast proliferation and differentiation (39, 40). Interestingly, an increase of $[Ca^{2+}]_i$ in UMR-106 cells antagonizes the antiproliferative effect of cAMP, suggesting a role for Ca^{2+} in the regulation of cell growth (34). Aside from PTH, 1,25-$(OH)_2$-vitamin D_3, mechanical stress, estradiol, and testosterone cause rapid Ca^{2+} influx into osteoblasts through plasma membrane Ca^{2+} channels (5, 10, 26, 41–44). The modulation of Ca^{2+} channel activity in osteoblasts by many factors that regulate bone metabolism suggests an important role for the Ca^{2+} signaling pathway in bone physiology.

We thank Ms. B. Coutermarsh for excellent technical assistance. These studies were funded by National Institutes of Health Grants R01GM34399 and R01ES05860 to P.A.F. and R01NS27504 to S.C.F., and by a gift from Miles Laboratories. E.L.R.B. was supported by Training Grant DK07301 from the National Institute of Diabetes and Digestive and Kidney Diseases (NIDDK). Bovine PTH-(1–84) was obtained through National Hormone and Pituitary Program, NIDDK, National Institute of Child Health and Human Development, and United States Department of Agriculture.

1. Hofmann, F., Biel, M. & Flockerzi, V. (1994) *Annu. Rev. Neurosci.* **17,** 399–418.
2. Spedding, M. & Paoletti, R. (1992) *Pharmacol. Rev.* **44,** 363–376.
3. Perez-Reyes, E. & Schneider, T. (1994) *Drug Dev. Res.* **33,** 295–318.
4. Yamaguchi, D. T., Hahn, T. J., Iida-Klein, A., Kleeman, C. R. & Muallem, S. (1987) *J. Biol. Chem.* **262,** 7711–7718.
5. Lieberherr, M. (1987) *J. Biol. Chem.* **262,** 13168–13173.
6. Guggino, S. E., Lajeunesse, D., Wagner, J. A. & Snyder, S. H. (1989) *Proc. Natl. Acad. Sci. USA* **86,** 2957–2960.
7. Guggino, S. E., Wagner, J. A., Snowman, A. M., Hester, L. D., Sacktor, B. & Snyder, S. H. (1988) *J. Biol. Chem.* **263,** 10155–10161.
8. Yamaguchi, D. T., Green, J., Kleeman, C. R. & Muallem, S. (1989) *J. Biol. Chem.* **264,** 197–204.
9. Karpinski, E., Wu, L., Civitelli, R., Avioli, L. V., Hruska, K. A. & Pang, P. K. T. (1989) *Calcif. Tissue Int.* **45,** 54–57.
10. Duncan, R. & Misler, S. (1989) *FEBS Lett.* **251,** 17–21.
11. Morain, P., Peglliion, J.-L. & Giesen-Crouse, E. (1992) *Eur. J. Pharmacol.* **220,** 11–17.
12. Chesnoy-Marchais, D. & Fritsch, J. (1988) *J. Physiol. (London)* **398,** 291–311.
13. Barry, E. L. R. & Friedman, P. A. (1993) *J. Bone Miner. Res.* **8,** S362 (abstr.).
14. Partridge, N. C., Alcorn, D., Michelangeli, V. P., Ryan, G. & Martin, T. J. (1983) *Cancer Res.* **43,** 4308–4314.
15. Tanabe, T., Takeshima, H., Mikami, A., Flockerzi, V., Takahashi, H., Kangawa, K., Kojima, M., Matsuo, H., Hirose, T. & Numa, S. (1987) *Nature (London)* **328,** 313–318.
16. Snutch, T. P., Tomlinson, W. J., Leonard, J. P. & Gilbert, M. M. (1991) *Neuron* **7,** 45–57.
17. Hui, A., Ellinor, P. T., Krizanova, O., Wang, J.-J., Diebold, R. J. & Schwartz, A. (1991) *Neuron* **7,** 35–44.
18. Barry, E. L. R., Gesek, F. A. & Friedman, P. A. (1993) *BioTechniques* **15,** 1016–1020.
19. Gesek, F. A. & Friedman, P. A. (1992) *J. Clin. Invest.* **90,** 429–438.
20. Mikami, A., Imoto, K., Tanabe, T., Niidome, T., Mori, Y., Takeshima, H., Narumiya, S. & Numa, S. (1989) *Nature (London)* **340,** 230–233.
21. Koch, W. J., Ellinor, P. T. & Schwartz, A. (1990) *J. Biol. Chem.* **265,** 17786–17791.
22. Seino, S., Chen, L., Seino, M., Blondel, O., Takeda, J., Johnson, J. H. & Bell, G. I. (1992) *Proc. Natl. Acad. Sci. USA* **89,** 584–588.
23. Ellis, S. B., Williams, M. E., Ways, N. R., Brenner, R., Sharp, A. H., Leung, A. T., Campbell, K. P., McKenna, E., Koch, W. J., Hui, A., Schwartz, A. & Harpold, M. M. (1988) *Science* **241,** 1661–1664.
24. Malouf, N. N., McMahon, D. K., Hainsworth, C. N. & Kay, B. K. (1992) *Neuron* **8,** 899–906.
25. Yu, A. L., Hebert, S. C., Brenner, B. M. & Lytton, J. (1992) *Proc. Natl. Acad. Sci. USA* **89,** 10494–10498.
26. Caffrey, J. M. & Farach-Carson, M. C. (1989) *J. Biol. Chem.* **264,** 20265–20274.
27. Loza, J., Stephan, E., Dolce, C., Dziak, R. & Simasko, S. (1994) *Calcif. Tissue Int.* **55,** 128–133.
28. Snutch, T. P. & Reiner, P. B. (1992) *Curr. Biol.* **2,** 247–253.
29. Diebold, R. J., Koch, W. J., Ellinor, P. T., Wang, J.-J., Muthuchamy, M., Wieczorek, D. F. & Schwartz, A. (1992) *Proc. Natl. Acad. Sci. USA* **89,** 1497–1501.
30. Perez-Reyes, E., Wei, X., Castellano, A. & Birnbaumer, L. (1990) *J. Biol. Chem.* **265,** 20430–20436.
31. Chaudhari, N. (1992) *J. Biol. Chem.* **267,** 25636–25639.
32. Feron, O., Octave, J.-N., Christen, M.-O. & Godfraind, T. (1994) *Eur. J. Biochem.* **222,** 195–202.
33. Brawley, R. M. & Hosey, M. (1992) *J. Biol. Chem.* **267,** 18218–18223.
34. Yamaguchi, D. T., Hahn, T. J., Beeker, T. G., Kleeman, C. R. & Muallem, S. (1988) *J. Biol. Chem.* **263,** 10745–10753.
35. Yamaguchi, D. T., Kleeman, C. R. & Muallem, S. (1987) *J. Biol. Chem.* **262,** 14967–14973.
36. Dempster, D. W., Cosman, F., Parisien, M., Shen, V. & Lindsay, R. (1993) *Endocr. Rev.* **14,** 690–709.
37. Misra, R. P., Bonni, A., Miranti, C. K., Rivera, V. M., Sheng, M. & Greenberg, M. E. (1994) *J. Biol. Chem.* **269,** 25483–25493.
38. Thompson, M. A., Ginty, D. D., Bonni, A. & Greenberg, M. E. (1995) *J. Biol. Chem.* **270,** 4224–4235.
39. Grigoriadis, A. E., Schellander, K., Wang, Z. Q. & Wagner, E. F. (1993) *J. Cell Biol.* **122,** 685–701.
40. Kano, J., Sugimoto, T., Kanatani, M., Kuroki, Y., Tsukamoto, T., Fukase, M. & Chihara, K. (1994) *J. Cell. Physiol.* **161,** 358–366.
41. Yamaguchi, D. T., Green, J., Kleeman, C. R. & Muallem, S. (1989) *J. Biol. Chem.* **264,** 4383–4390.
42. Civitelli, R., Kim, Y. S., Gunsten, S. L., Fujimori, A., Huskey, M., Avioli, L. V. & Hruska, K. A. (1990) *Endocrinology* **127,** 2253–2262.
43. Lieberherr, M. & Grosse, B. (1994) *J. Biol. Chem.* **269,** 7217–7223.
44. Lieberherr, M., Grosse, B., Kachkache, M. & Balsan, S. (1993) *J. Bone Miner. Res.* **8,** 1365–1376.